OPEN ACCESS
Saudi Journal of Civil Engineering
Abbreviated Key Title: Saudi J Civ Eng
ISSN 2523-2657 (Print) |ISSN 2523-2231 (Online)
Scholars Middle East Publishers, Dubai, United Arab Emirates
Journal homepage: https://saudijournals.com/journal/sjce/home

Original Research Article

The Upshot of Nonlinear Thermal Emission on a Conducting Jeffrey Nanofluid Flow over a Stretching Sheet: A Lie Group Approach

Isah Bala Yabo[1], Michael Williams[1*], Aminu Mustafa[1] and Audu Ahamd[2]

[1]Department of Mathematics, Usmanu Danfodio University, Sokoto
[2]Department of Statistics, Usmanu Danfodio University, Sokoto

DOI: 10.36348/sjce.2023.v07i08.002 | **Received:** 23.04.2023 | **Accepted:** 10.06.2023 | **Published:** 25.09.2023

***Corresponding author:** Michael Williams
Department of Mathematics, Usmanu Danfodio University, Sokoto

Abstract

The upshot of nonlinear thermal radiation of steady state MHD heat transfer of Jeffrey nanofluid together with prescribed boundary conditions of interest was studied. Essential fluid properties, dimensionless switch parameters with the assistance of the Lie group method were used to transform the convenient partial differential equations that describe the present model into a system of ordinary differential equations. The generalized flow of the present model incorporates Jeffrey parameters and nonlinear thermal radiation. The Mathematical model is first renovated into ordinary differential equations by Lie symmetry group alteration. The renovated equations were solved numerically using a bvp4c MATLAB solver. The Jeffrey parameter serves as a stabilizer on the velocity of the fluid while thermal radiation parameter and heat source-sink parameter improves the flow temperature. Lewis number, chemical reaction parameter diminished the mass transfer flow. Equally skin friction, Sherwood number and Nusselt number were expanded.

Keywords: Jeffrey nanofluid, Lie group approach, heat source-sink and nonlinear thermal radiation.

1.0 INTRODUCTION

Lubricant, water, ethanol fuel, glycol and so on are instances of nanofluid which is a based fluid with dense minute sized particles which can also be seen as a way of accelerating the outcome of transfer of heat in liquids. Nanofluid can be applied on automobile engines and welding equipment to bring down the temperature of high heat flux devices such as high micro waves tubes. Nanofluid is applicable in so many industries which include nuclear reactors, transportation, microelectronics, fuel cells, biomedicine, food storage and domestic refrigerator engine. Lawal *et al*., [1] explored Powell nanoliquid in a vertical wall with impact of viscosity. They augured in their findings that temperature profiles escalate by boosting Brownian motion and thermophoresis and take the reverse case for concentration of the fluid. Bidemi and Ahamed [2] Scrutinized magnetohydrodynamic nanoliquid using a stretching sheet Aman *et al*., [3] Thrashed out Casson fluid flow of mixed convective heat transfer of multiwall carbon nanotube and single-wall carbon nanotube on a vertical sheet was performed analytically. Aman *et al*., [4] examined time fractional derivatives using convective magnetohydrodynamic nanofluid flow in a stretching surface. They believed that nanofluid can be used in factories to manufacture materials for solar energy. Abbas *et al*., [5] explored Rosseland approximation for thermal radiation and porous surfaces of nanoliquid in a parallel plate. Sobamowo [6] considered the effects of magnetohydrodynamic on nanoparticles along a stretching sheet. Das *et al*., [7] carried out magnetohydrodynamic heat transfer flow of nanoliquid along a parallel plate including Brownian motion and thermophoresis.

Origination for Jeffrey nanofluid has announced an entirely new trend to the investigators working in fluid mechanics. Muhammad *et al*., [8] Considered magnetohydrodynamic heat transfer of Jeffrey nanofluid using a parallel plate. To showcase the identity of nanofluid Brownian motion and Thermophoresis was used. Hayat *et al*., [9] presented convective conditions of magnetohydrodynamic of Jeffrey nanoliduid on a vertical plate. Reddy and Makinde [10] considered MHD flow of Jeffrey nanofluid in parallel plates. They used wavelength assumptions to change the system of partial differential equations to ordinary differential equations. Waqas *et*

al., [11] reported linear thermal radiation with external heat source-sink of Jeffrey nanofluid on a vertical channel. Abbasi *et al*., [12] equipped the MHD Jeffrey nanoliquid using thermophoresis and Brownian motion in the flow.

Countless investigators' attention has been drowned on nonlinear thermal radiation as a consequence of its application in engineering works. However, nonlinear thermal radiation is very significant in processing industries that make use of heat to obtain a good end product. This end product can be used to produce gas turbines and plants for electricity generation etc. Ahmad *et al*., [13] scrutinized the effect of Maxwell nanoliquid on a vertical channel with chemical reaction and linear thermal radiation. In addition, their upshot is used in boosting transfer of heat, energy derived from solar, structures of transportation and so on. Jha and Samaila [14] carried out the significance of nonlinear thermal radiation and thermophoresis on a heat and mass transfer of mixed convective vertical channels. The fluid temperature is enhanced by raising the values of radiative heat flux which in turn causes the velocity and concentration closed to the porous surface to goes up. Khan *et al*., [15] examined the importance of nonlinear thermal radiation in a walter-B nanofluid by make used of thermophoresis, Brownian motion and convective boundary conditions. Their outcome shows that escalating Schmidt number reduced the concentration of nanofluid. Ilias *et al*., [16] investigated the magnetohydrodynamic transfer of heat on a parallel plate. Their outcome exposed how transfer of heat and fluid flow upset the leading surface.

This recent work intends to improve the work of Ahmad *et al*., 13] by incorporating Jeffrey parameter and nonlinear thermal radiation in the fluid flow. However, the partial differential equations were changed to ordinary differential equations with the help of Lie group approach and the renovated problems were solved numerically using bvp4c MATLAB solver.

2.0 MATHEMATICAL FORMULATION

A transfer of heat and mass of a steady state MHD of Jeffrey nanofluid with nonlinear thermal radiation whose liquid is electrically viscous and incompressible, the $B(x)=\frac{B_0}{\sqrt{x}}$ is the transverse magnetic field, and $V(x)$ is the momentum of suction/injection, the energy wall is represented with T_w and the wall of concentration is C_w, from the channel, according to figure 1, x-direction is the assumption for the flow. Also chemical reactions (γ) were also considered. The induced magnetic field is irrelevant in relationship with the external magnetic field.

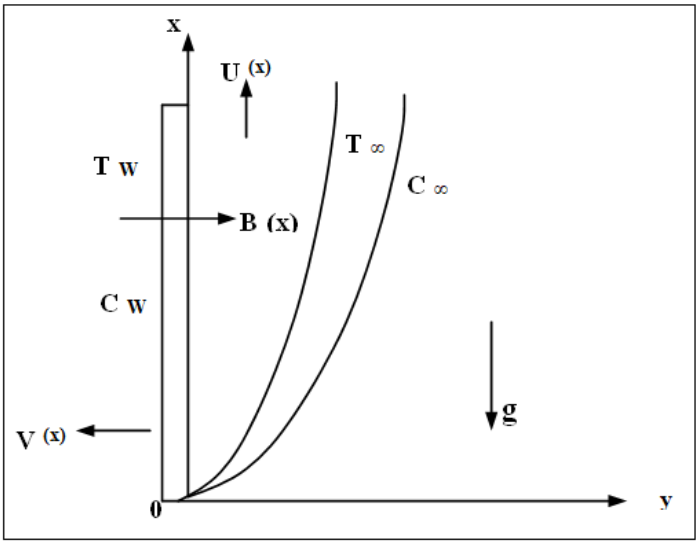

Figure 1: Geometry of the flow channel

2.1 Mathematical Model

Applying the Boussinesq approximations we obtain the following governing equations as Ahmad *et al*., [13].

$$\frac{\partial u}{\partial x}+\frac{\partial v}{\partial y}=0 \ldots\ldots\ldots\ldots\ldots\ldots (1)$$

$$u\frac{\partial u}{\partial x}+v\frac{\partial u}{\partial y}+\frac{\lambda_1}{1+\lambda}\left[u^2\frac{\partial^2 u}{\partial x^2}+v^2\frac{\partial^2 u}{\partial y^2}+2uv\frac{\partial^2 u}{\partial x\partial y}\right]=$$

$$\frac{V}{1+\lambda}\frac{\partial^2 u}{\partial y^2}+\left[(1-C_\infty)\rho_{f_\infty}\beta(T-T_\infty)-(\rho_p-\rho_{f_\infty})(C-C_\infty)\right]g-\frac{\sigma B^2(x)}{\rho_f}\left[u+\lambda_1 vu\frac{\partial u}{\partial y}\right] \quad \text{..... (2)}$$

$$u\frac{\partial T}{\partial x}+v\frac{\partial T}{\partial y}=\frac{\kappa}{(\rho c)_f}\frac{\partial^2 T}{\partial y^2}-\frac{1}{(\rho c)_f}\frac{\partial q_r}{\partial y}+\frac{Q}{(\rho c)_f}(T-T_\infty)+\tau\left[D_B\frac{\partial C}{\partial y}\frac{\partial T}{\partial y}+\frac{D_T}{T_\infty}\left(\frac{\partial T}{\partial y}\right)^2\right] \quad \text{..... (3)}$$

$$u\frac{\partial C}{\partial x}+v\frac{\partial C}{\partial y}=D_B\frac{\partial^2 C}{\partial y^2}+\frac{D_T}{T_\infty}\frac{\partial^2 T}{\partial y^2}-R(C-C_\infty) \quad \text{..... (4)}$$

The boundary conditions for the above models are as follow:

$$\left.\begin{aligned} &u=U_w(x)=C_1xv=v_w(x), \quad T=\frac{-k\partial T}{\partial y}=hf\left(T_f-T\right), \quad C=C_w \quad at \quad y=0\\ &u\to 0, \quad T\to T_\infty, \quad C\to C_\infty \quad \text{as} \quad y\to\infty \end{aligned}\right\} \quad \text{..... (5)}$$

Using Rosseland approximation, the radiative heat flux term q_r along y is expressed as follows

$$q_r=-\frac{4\sigma_1}{3k_1}\frac{\partial T^4}{\partial y} \quad \text{..... (6)}$$

In order to linearized equation (6), expand T^4 about T_∞ into Taylor's series expansion gives

$$T^4=\left(\frac{T-T_\infty}{T_w-T_\infty}(T_1-T_0)+T_0\right)^4 \quad \text{..... (7)}$$

Substitute equation (6) and (7) into equation (3) we get

$$u\frac{\partial T}{\partial x}+v\frac{\partial T}{\partial y}=\left[1+\frac{4N}{3}\left(C_T+\frac{T-T_\infty}{T_w-T_\infty}\right)^3\right]\frac{\partial^2 T}{\partial y^2}+4N\left[C_T+\frac{T-T_\infty}{T_w-T_\infty}\right]^2\left(\frac{\partial T}{\partial y}\right)^2$$

$$+\frac{Q}{(\rho c)_f}(T-T_\infty)+\tau\left[D_B\frac{\partial C}{\partial y}\frac{\partial T}{\partial y}+\frac{D_T}{T_\infty}\left(\frac{\partial T}{\partial y}\right)^2\right] \quad \text{..... (8)}$$

2.2 Stream Function and Non- dimensional Variables

Using stream function ψ, defined by

$$v=-\frac{\partial\psi}{\partial x} \text{ and } u=\frac{\partial\psi}{\partial y} \quad \text{..... (9)}$$

Together with non- dimensional variables

$$\left.\begin{aligned} &\theta=\frac{T-T_\infty}{T_w-T_\infty}, \quad \phi=\frac{C-C_\infty}{C_w-C_\infty}, \quad \Pr=\frac{4r^2}{(\rho c)_f}, \quad M^2=\frac{\sigma B_0^2}{\rho_f}, \quad Ra=\frac{(1-\phi_\infty)\beta g\Delta\theta}{V},\\ &Le=\frac{\alpha}{D_b}, \quad Nr=\frac{(\rho_p-\rho_{f_\infty})\Delta\phi}{\rho_{f_\infty}\beta\Delta\theta(1-\phi_\infty)}, \quad Nb=\frac{D_B\Delta\phi(\rho c)_p}{\kappa}, \quad Nt=\frac{D_T\Delta\theta(\rho c)_p}{\kappa T_\infty},\\ &N=\frac{4T_\infty^3\sigma_1}{\mathrm{K}_1\kappa}, \quad \gamma=\frac{Uk}{D_B}, \quad \beta=\lambda_1C_1, \quad Q=\frac{Q}{(\rho c)_f}, \quad x=\frac{C_1}{U_1}x, \quad y=\sqrt{\frac{C_1}{v}}y, \quad u=\frac{u}{U_1} \end{aligned}\right\} \quad \text{..... (10)}$$

Substitute equations (9) and (10) into equations (1), (2), (4), (5) and (8), note that equation (1) is satisfied identically. Hence the following are obtained:

$$(1+\lambda)\left[\frac{\partial\psi}{\partial y}\frac{\partial^2\psi}{\partial x\partial y}-\frac{\partial\psi}{\partial x}\frac{\partial^2\psi}{\partial y^2}\right]+\beta\left[\left(\frac{\partial\psi}{\partial y}\right)^2\frac{\partial^3\psi}{\partial x^2\partial y}-\left(\frac{\partial\psi}{\partial x}\right)^2\frac{\partial^3\psi}{\partial y^3}-2\frac{\partial\psi}{\partial y}\frac{\partial\psi}{\partial x}\frac{\partial^3\psi}{\partial x\partial y^2}\right]=$$

$$\frac{\partial^3\psi}{\partial y^3}+(1+\lambda)Ra[\theta-N_r\phi]-(1+\lambda)M^2\left(\frac{\partial\psi}{\partial y}-\beta\frac{\partial\psi}{\partial x}\frac{\partial^2\psi}{\partial y^2}\right) \quad \ldots\ldots\ldots\ldots\ldots\ldots (11)$$

$$\Pr\left[\frac{\partial\psi}{\partial y}\frac{\partial\theta}{\partial x}-\frac{\partial\psi}{\partial x}\frac{\partial\theta}{\partial y}\right]=\left[1+\frac{4N}{3}(C_T+\theta)^3\right]\frac{\partial^2\theta}{\partial y^2}+4N[C_T+\theta]^2\left(\frac{\partial\theta}{\partial y}\right)^2$$

$$+Q\theta+N_b\frac{\partial\phi}{\partial y}\frac{\partial\theta}{\partial y}+N_t\left(\frac{\partial\theta}{\partial y}\right)^2 \quad \ldots\ldots\ldots\ldots\ldots (12)$$

$$Le\left[\frac{\partial\psi}{\partial y}\frac{\partial\phi}{\partial x}-\frac{\partial\psi}{\partial x}\frac{\partial\phi}{\partial y}\right]=\frac{\partial^2\phi}{\partial y^2}+\frac{N_t}{N_b}\frac{\partial^2\theta}{\partial y^2}-\gamma\phi \quad \ldots\ldots\ldots\ldots\ldots\ldots (13)$$

Where all the symbols are well defined on Table 2.1.

The boundary condition becomes

$$\left.\begin{aligned}&\frac{\partial\psi}{\partial y}=x,\quad -\frac{\partial\psi}{\partial x}=\frac{V_w}{\sqrt{C_1 v}},\quad \theta=-B_i(1-\theta),\quad \phi=1\quad at\quad y=0\\&\frac{\partial\psi}{\partial y}\to 0,\quad \theta\to 0,\quad \phi\to 0\quad \text{as}\quad y\to\infty\end{aligned}\right\} \quad \ldots\ldots\ldots\ldots\ldots\ldots (14)$$

Table 2.1: Nomenclature

Symbol	Description
Pr	Prandtl number
Ra	Rayleigh number
Nr	Buoyancy ratio
Nt	Thermophoresis parameter
B_0	Magnetic field strength
u, v	Velocity components along x, y-axis
$(\rho c)_p$	Nanoparticles specific heat
$\tau=\frac{(\rho c)_p}{(\rho c)_f}$	Heat capacity ratio
C	Nanoparticles concentration
K^*	Mean absorption coefficient
T_∞	Ambient liquid temperature
$(\rho c)_f$	Fluid specific heat
β	Deborah number
S	Mass transfer parameter
M	Hartmann number
Le	Lewis number
Nb	Brownian motion parameter
N	Thermal radiation parameter

Symbol	Description
ρ_f	Density of base fluid
T	Temperature variable
C_∞	Ambient liquid concentration
σ_1	Stefan-Boltzmann constant
$\alpha = \frac{k}{(\rho c)_f}$	Thermal diffusivity
k_1	Absorption coefficient
Q	Heat source/sink
Bi	Biot number
Ct	Temperature ratio
Greek Symbols	
Symbol	**Description**
γ	Chemical reaction parameter
ν	Kinematic viscosity
λ_1	Relaxation parameter
σ	Electrical conductivity
λ	Jeffrey parameter

2.3 Lie Group Exploration

Following the classical Lie group approach (Ahmed *et al*., [13] and Das *et al*., [7]) the special scaling group transformations of equations (11) – (13) and (14) are defined by the following:

$$\Gamma:\ x^* = xe^{\varepsilon\alpha_1}, y^* = ye^{\varepsilon\alpha_2}, \psi^* = \psi e^{\varepsilon\alpha_3}, \theta^* = \theta e^{\varepsilon\alpha_4}, \phi^* = \phi e^{\varepsilon\alpha_5} \quad \text{..... (15)}$$

By putting equation (15) into equation (11) – (13) yield's the following which transformed coordinates $(x, y, \psi, \theta, \phi)$ to $(x^*, y^*, \psi^*, \theta^*, \phi^*)$, where ε is parameter of the group and α is the real number.

$$e^{\varepsilon(2\alpha_2+\alpha_1-2\alpha_3)}(1+\lambda)\left[\frac{\partial\psi}{\partial y}\frac{\partial^2\psi}{\partial x\partial y} - \frac{\partial\psi}{\partial x}\frac{\partial^2\psi}{\partial y^2}\right] + \beta e^{\varepsilon(2\alpha_1+3\alpha_2-3\alpha_3)}\left[\left(\frac{\partial\psi}{\partial y}\right)^2\frac{\partial^3\psi}{\partial x^2\partial y} + \left(\frac{\partial\psi}{\partial x}\right)^2\frac{\partial^3\psi}{\partial y^3} - 2\frac{\partial\psi}{\partial y}\frac{\partial\psi}{\partial x}\frac{\partial^3\psi}{\partial x\partial y^2}\right]$$

$$= e^{\varepsilon(3\alpha_2-\alpha_3)}\frac{\partial^3\psi}{\partial y^3} + e^{-\varepsilon\alpha_4}\left[(1+\lambda)Ra\theta\right] - e^{-\varepsilon\alpha_5}\left[(1+\lambda)RaN_r\phi\right] -$$

$$(1+\lambda)M^2\left[e^{\varepsilon(\alpha_2-\alpha_3)}\frac{\partial\psi}{\partial y} - e^{\varepsilon(\alpha_1+2\alpha_2-2\alpha_3)}\right] \quad \text{..... (16)}$$

$$e^{\varepsilon(\alpha_1+\alpha_2-\alpha_3-\alpha_4)}\Pr\left[\frac{\partial\psi}{\partial y}\frac{\partial\theta}{\partial x} - \frac{\partial\psi}{\partial x}\frac{\partial\theta}{\partial y}\right] = e^{\varepsilon(2\alpha_2-4\alpha_4)}\left[1+\frac{4}{3}N(C_T-\theta)^3\right]\frac{\partial^2\theta}{\partial y^2} +$$

$$+e^{\varepsilon(2\alpha_2-4\alpha_4)}4N[C_T+\theta]^2\left(\frac{\partial\theta}{\partial y}\right)^2 + e^{\varepsilon(-\alpha_4)}Q\theta + e^{\varepsilon(2\alpha_2-\alpha_4-\alpha_5)}N_b\frac{\partial\phi}{\partial y}\frac{\partial\theta}{\partial y} + e^{\varepsilon(2\alpha_2-2\alpha_4)}N_t\left(\frac{\partial\theta}{\partial y}\right)^2$$

..... (17)

$$e^{\varepsilon(\alpha_1+\alpha_2-\alpha_3-\alpha_5)}Le\left[\frac{\partial\psi}{\partial y}\frac{\partial\phi}{\partial x} - \frac{\partial\psi}{\partial x}\frac{\partial\phi}{\partial y}\right] = e^{\varepsilon(2\alpha_2-\alpha_5)}\frac{\partial^2\phi}{\partial y^2} + e^{\varepsilon(2\alpha_2-\alpha_4)}\frac{N_t}{N_b}\frac{\partial^2\theta}{\partial y^2} - e^{-\varepsilon(\alpha_5)}\gamma\phi \quad \text{..... (18)}$$

By comparing various exponential terms of equations (16) - (18) the invariant of the system is achieved as obtained below:

$$\left.\begin{aligned} &2\alpha_2+\alpha_1-2\alpha_3=2\alpha_1+\alpha_2-3\alpha_3=3\alpha_2-\alpha_3=-\alpha_4=-\alpha_5=\alpha_2-\alpha_3=\alpha_1+2\alpha_2-2\alpha_3=\alpha_2-\alpha_3\\ &\alpha_1+\alpha_2-\alpha_3-\alpha_4=2\alpha_2-4\alpha_4=2\alpha_2-4\alpha_4=-\alpha_4=2\alpha_2-\alpha_4-\alpha_5=2\alpha_2-2\alpha_4\\ &\alpha_1+\alpha_2-\alpha_3-\alpha_5=2\alpha_2-\alpha_5=2\alpha_2-\alpha_4=-\alpha_5 \end{aligned}\right\} \quad \ldots\ldots 19$$

From equation (14) the invariance of the boundary conditions becomes:

$$\alpha_1=\alpha_3, \qquad \alpha_2=\alpha_4=\alpha_5=0 \quad \ldots\ldots\ldots\ldots\ldots\ldots (20)$$

Subject to the solutions of equation (19) using equation (20) the groups of transformations (15) take the form:

$$\Gamma:\ x^*=xe^{\varepsilon\alpha_1},\ \ y^*=y,\ \psi^*=\psi e^{\varepsilon\alpha_1}, \qquad \theta^*=\theta, \qquad \phi^*=\phi \quad \ldots\ldots\ldots\ldots (21)$$

Also, employing Taylor series expansions yields:

$$\left.\begin{aligned} &x^*-x=\varepsilon x\alpha_1+0(\varepsilon^2)\\ &y^*-y=0\\ &\psi^*-\psi=\varepsilon\psi\alpha_1+0(\varepsilon^2)\\ &\theta^*-\theta=0\\ &\phi^*-\phi=0 \end{aligned}\right\} \quad \ldots\ldots\ldots\ldots\ldots (22)$$

Since $\alpha_1\neq 0$, rewrite equation (22) to give the following characteristic equations

$$\frac{x^*-x}{x\alpha_1}=\varepsilon, \qquad y^*-y=0, \qquad \frac{\psi^*-\psi}{\psi\alpha_1}=\varepsilon, \qquad \theta^*-\theta=0,\ \ \phi^*-\phi=0 \quad \ldots\ldots\ldots\ldots (23)$$

Now, in terms of differentials equation (23) becomes:

$$\frac{d\psi*}{\alpha_1\psi^*}=\frac{dx^*}{x^*\alpha_1} \quad \ldots\ldots\ldots\ldots\ldots\ldots (24)$$

$$dy^*=d\theta^*=d\phi^*=0 \quad \ldots\ldots\ldots\ldots\ldots\ldots (25)$$

By integrating equation (24) – (25) the following similarity transformations were determined:

$$y^*=\eta,\ \ \psi^*=x^*f(\eta),\ \ \theta^*=\theta(\eta) \text{ and } \phi^*=\phi(\eta) \quad \ldots\ldots\ldots\ldots\ldots\ldots (26)$$

Where $\eta,\ \ f(\eta),\ \ \theta(\eta),$ and $\phi(\eta)$ are constant

Employing equation (26) into equations (11) – (14), the equations below emerged:

$$f'''+(1+\lambda)\left[ff''-f'^2\right]-\beta\left[f^2f'''-2fff''\right]-(1+\lambda)\left[M^2\left(f'-\beta ff''\right)\right]+(1+\lambda)Ra\left[\theta-N_r\phi\right]=0$$

$$\ldots\ldots\ldots\ldots (27)$$

$$\left[1+\frac{4}{3}N\left(C_T+\theta\right)^3\right]\theta''+4N\left[C_T+\theta\right]^2\theta'^2+\Pr\left[f\theta'+Q\theta+N_b\phi'\theta'+N_t\theta'^2\right]=0 \quad \ldots\ldots\ldots\ldots (28)$$

$$\phi''+\frac{N_t}{N_b}\theta''+Le\left[f\phi'-\gamma\phi\right]=0 \quad \ldots\ldots\ldots\ldots\ldots\ldots (29)$$

While the boundary conditions reads:

$$\left.\begin{aligned} &f=S,\ \ f'=1,\ \ \theta'=-B_i\left(1-\theta\right),\ \ \phi=1 \quad \text{at} \quad \eta=0\\ &f'\to 0,\ \ \theta\to 0,\ \ \phi\to 0 \quad \text{as} \quad \eta\to\infty \end{aligned}\right\} \quad \ldots\ldots\ldots\ldots\ldots (30)$$

2.4 Physical Quantities

The interested physical term are the reduced Skin friction coefficients $\left(C_f\right)$, the reduced Nusselt number $\left(Nur\right)$ and reduced Sherwood number $\left(Shr\right)$:

$$C_f = \frac{1}{2}\mathrm{Re}_x^{-1/2} C_f = f''(0) \ldots\ldots\ldots\ldots (31)$$

$$Nur = \mathrm{Re}_x^{-1/2} Nu = -\theta'(0) \ldots\ldots\ldots\ldots (32)$$

$$Shr = \mathrm{Re}_x^{-1/2} Sh = -\phi'(0) \ldots\ldots\ldots\ldots (33)$$

The suites of equation (27) - (30) are solved numerically with bvp4c MATLAB solver. To ensure authenticity of the existent result, in the absence of Jeffrey parameter, the present work coincides with that of Hayat *et al*., [17], Turkyilmazoglu [18] and Ahmad *et al*., [13]. The assorted values of the reduced skin friction $f''(0)$ have been calculated for $\beta = Ra = S = Bi = \lambda = 0$ from table (3.1) which illustrates numerous values for Hartmann number. From the table below, our result with Ahmad *et al*., [13] established a brilliant agreement. So, it defends the use of the existing numerical results for present work.

3.0 Numerical Method and Result Validation

Table 3.1: Evaluation of the outcomes for the reduced skin friction $f''(0)$ with previous work

M	Hayat *et al*., [17]	Turkyilmazoglu [18]	Ahmad *et al*., [13]	Present Results
0.0	-1.00000	- 1.00000	-1.00000	-1.000000000
0.5	-1.224747	-1.224744	-1.224745	-1.224744871
1.0	-1.414217	-1.414213	-1.414215	-1.414213562

4.0 RESULTS AND DISCUSSION

This exact fragment is allotted to scrutinize a stable state magnetohydrodynamics heat transfer of some Jeffrey Nanofluid with nonlinear thermal radiation. In this studied, the default values are $Nr = \frac{1}{2}$, $N = \frac{1}{100}$, $S = \frac{1}{10}$, $Ra = \frac{1}{100}$, $Le = \frac{1}{5}$, $M^2 = \frac{1}{5}$, $Nt = \frac{1}{5}$, $\gamma = \frac{1}{10}$, $\mathrm{Pr} = \frac{71}{100}$, $\lambda = \frac{1}{2}$, $Nb = \frac{1}{5}$, $k = \frac{1}{2}$, $\beta = \frac{1}{5}$, $C_T = \frac{1}{5}$, $Q = \frac{1}{100}$, $Bi = \frac{1}{10}$. Unless otherwise detailed.

However, Figure (2-4) illustrate the upshot of velocity outline for different values of Jeffrey parameter $\left(\lambda\right)$ Hartmann number $\left(M\right)$ and Rayleigh number $\left(Ra\right)$ respectively. By enhancing the values of Rayleigh number $\left(Ra\right)$ the velocity of Jeffrey nanofluid goes up and the opposite direction is noticed for raising Jeffrey parameter $\left(\lambda\right)$ and Hartmann number $\left(M\right)$. Physically, Rayleigh number $\left(Ra\right)$ is the quotient of Buoyancy to the product of viscous and heat diffusion. An increase in Jeffrey parameter $\left(\lambda\right)$ indicates weaker retardation time. Hartmann number $\left(M\right)$ yields Lorentz force, such force triggered a confrontation in the flow Jeffrey nanofluid.

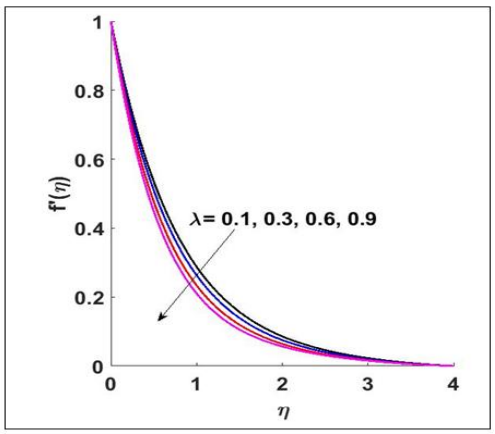

Figure 2: Velocity contours $\left(f'(\eta)\right)$ for Jeffrey parameter $\left(\lambda\right)$

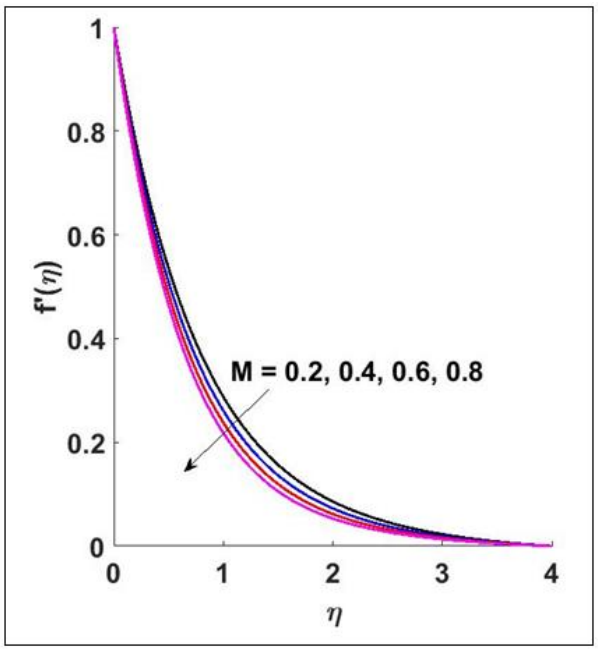

Figure 3: Velocity contours $\left(f'(\eta)\right)$ for Hartmann number $\left(M\right)$

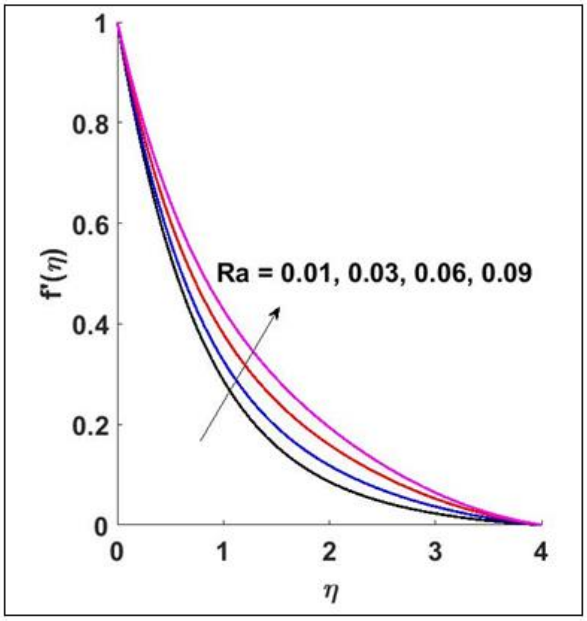

Figure 4: Velocity contours $\left(f'(\eta)\right)$ for Rayleigh number $\left(Ra\right)$

In addition, Figure (5-7) displays the consequence of heat source-sink parameter $\left(Q\right)$, temperature ratio $\left(Ct\right)$ and Biot number $\left(Bi\right)$ on temperature contours. The increase in heat source-sink parameter $\left(Q\right)$ Figure (5), temperature ratio $\left(Ct\right)$ Figure (6) and Biot number $\left(Bi\right)$ Figure (7) lead to increase in temperature outline. Generally, more heat is produced by escalating temperature ratio $\left(Ct\right)$. The heat transfer occurrence is improved by the presence of external heating source. Biot number $\left(Bi\right)$ signifies the quotient of conductive resistance in solids to the connective resistance in thermal boundary layer.

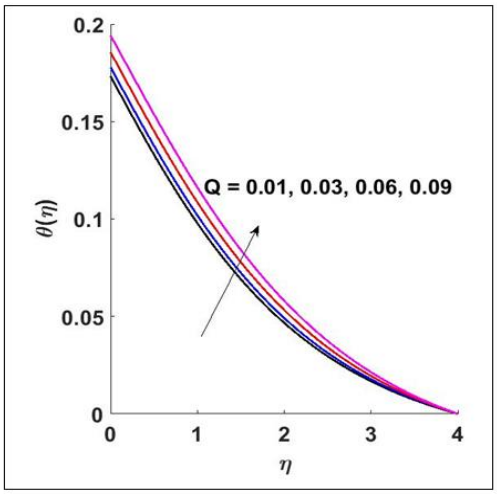

Figure 5: Temperature contours $\left(\theta\left(\eta\right)\right)$ for heat source-sink $\left(Q\right)$

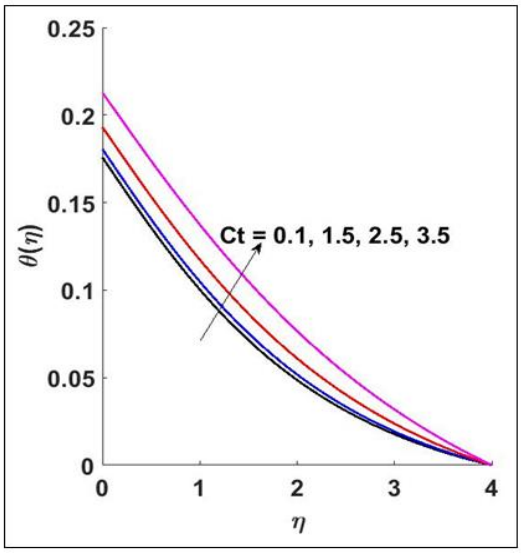

Figure 6: Temperature contours $\left(\theta\left(\eta\right)\right)$ for temperature ratio $\left(Ct\right)$

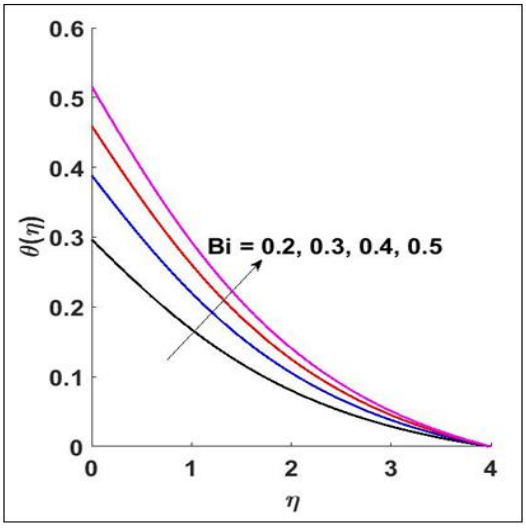

Figure 7: Temperature contours $\left(\theta\left(\eta\right)\right)$ for Biot number $\left(Bi\right)$

Furthermore, Figures (8 – 9) depict the results of concentration profile for different values of chemical reaction parameter (γ) and Lewis number (Le) respectively. The concentration profile goes down by raising the values of Lewis number (Le) and chemical reaction parameter (γ). Chemical reaction parameter (γ) outcomes in a condensed concentration boundary layer due to condensed species concentration. Physically, Lewis number (Le) is a quotient of thermal diffusivity to the mass diffusivity.

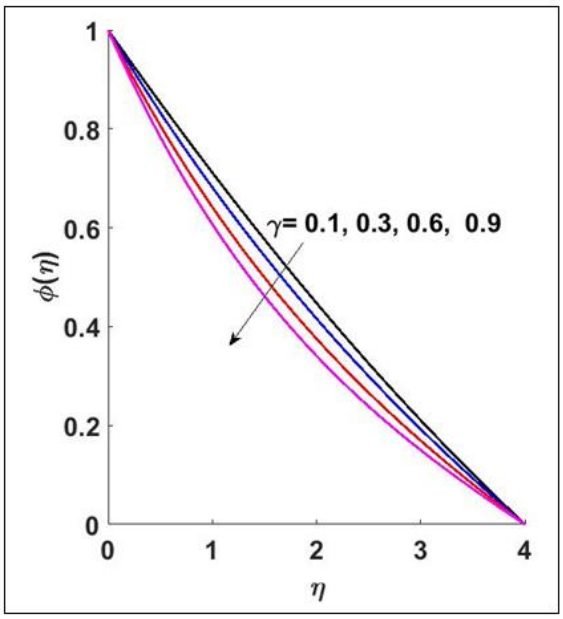

Figure 8: Concentration contours $(\phi(\eta))$ for chemical reaction (γ)

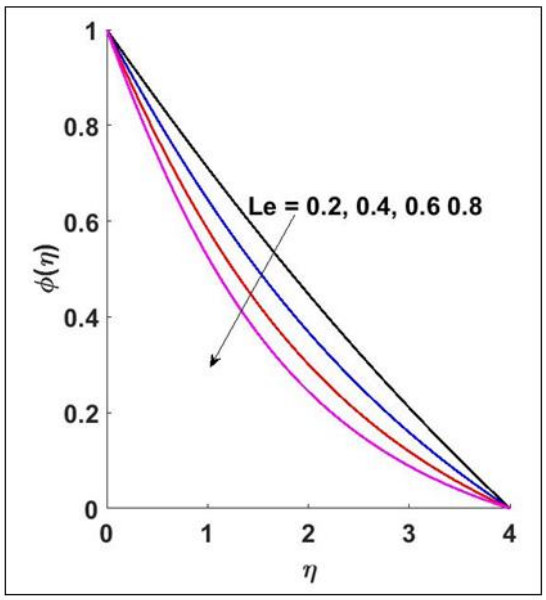

Figure 9: Concentration contours $(\phi(\eta))$ for Lewis number (Le)

Furthermore, the influence of Jeffrey parameter (λ) and Hartmann number (M) on skin friction is disclosed in figure (10) and (11) respectively. By boosting Jeffrey parameter (λ) and Hartmann number (M) the skin friction is diminished. Generally, the nanofluids are to some extent depressed

as Jeffrey parameter (λ) is enlarged. Likewise, the use of Hartmann number (M) yields Lorentz force, such strength triggered a struggle in the Jeffrey nanofluid flow which decline the viscosity of momentum boundary layer.

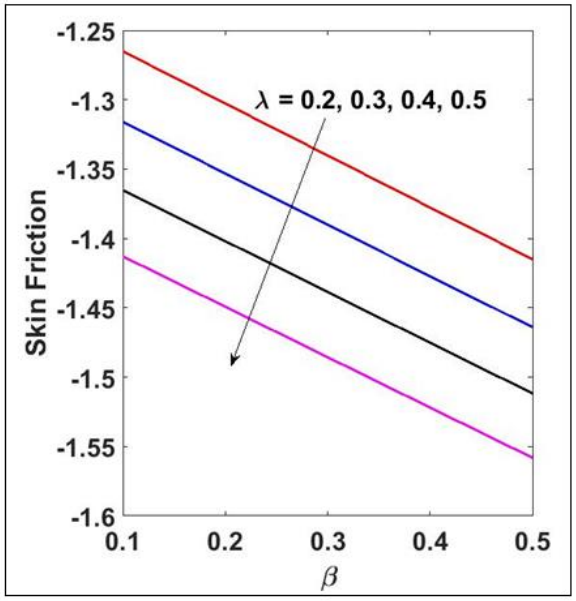

Figure 10: Skin frictions for Jeffrey parameter (λ)

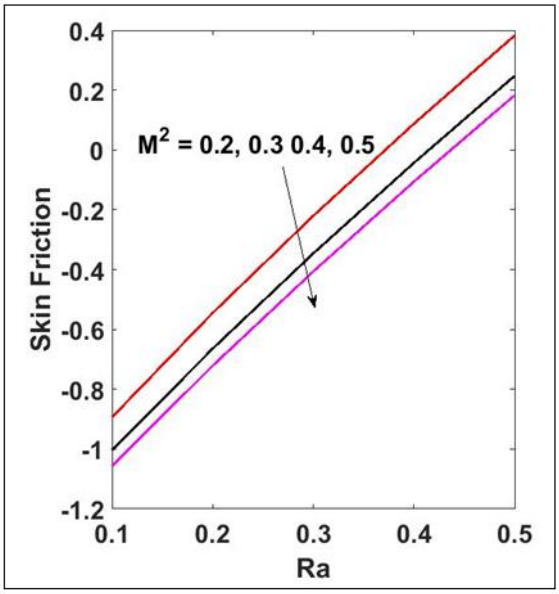

Figure 11: Skin frictions for Hartmann number (M)

Also, the effect of Brownian motion (Nb) and Biot number (Bi) on Nusselt number is notice in Figure (12) and (13) respectively. By strengthen Brownian motion (Nb) the Nusselt number goes down whereas the opposite situation is notice for Biot number (Bi). This drop is in line for nanoparticles of extraordinary thermal conductivity being driven away from the warm area to the motionless fluid.

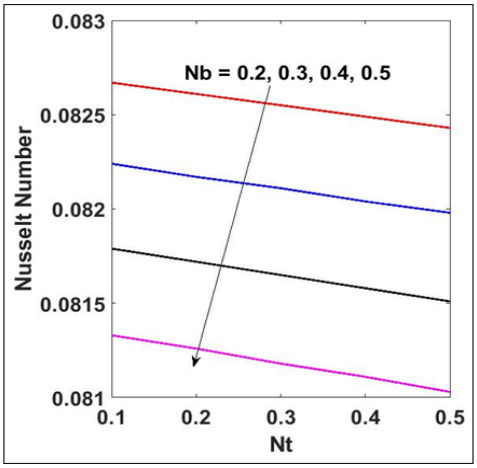

Figure 12: Nusselt number for Brownian motion (Nb)

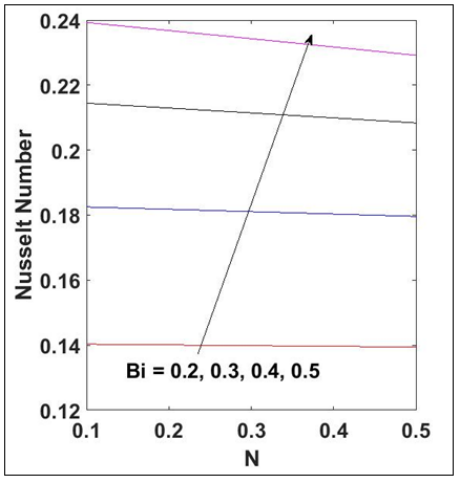

Figure 13: Nusselt number for Biot number (Bi)

Likewise, the product of Brownian motion (Nb) and Biot number (Bi) on Sherwood number is notice in Figure (14) and (15) respectively. The Sherwood number goes up by enhancing Brownian motion (Nb) and takes opposite direction for Biot number (Bi).

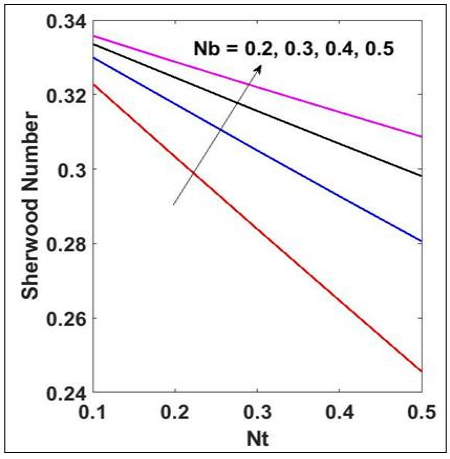

Figure 14: Sherwood number for Brownian motion (Nb)

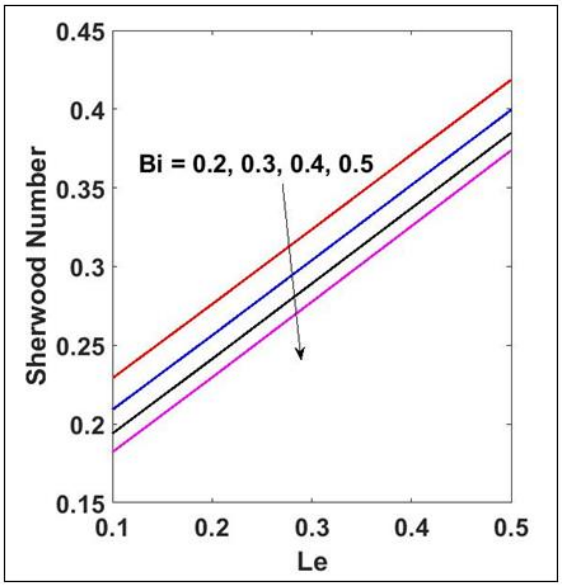

Figure 15: Sherwood number for Biot number (Bi)

5.0 CONCLUSION

The mathematical exploration on transfer of heat of Jeffrey nanofluid laminar boundary flow of a perpendicular plate inclined by viscous dissipation was investigated. The renovated equations were solved numerically. Some of the verdicts are:

i. The strength of Jeffrey parameter (λ) and Hartmann number (M) slows down the velocity of the Jeffrey nanofluid and is enhanced with Rayleigh number (Ra)

ii. By boosting temperature ratio parameter (Ct), heat source-sink parameter (Q) and Biot number (Bi) the flow of temperature is improved

iii. By escalating chemical reaction (γ), Lewis number (Le) diminished the concentration of the Jeffrey nanofluid

iv. The skin friction is diminished by enhancing Jeffrey parameter (λ) and Hartmann Number (M)

v. By raising Brownian motion (Nb) reduces the Nusselt number and took the reverse case for Biot number (Bi)

vi. The Sherwood number goes up by enhancing Brownian motion (Nb) and goes down by escalating Biot number (Bi)

REFERENCES

1. Lawal, M. O., Kasali, K. B., Ogunseye, H. A., Oni, M. O., Tijani, Y. O., & Lawal, Y. T. (2022). On the mathematical model of Eyring–Powell nanofluid flow with non-linear radiation, variable thermal conductivity and viscosity. *Partial Differential Equations in Applied Mathematics*, *5*, 100318.
2. Bidemi, O. F., & Ahamed, M. S. (2019). Soret and Dufour effects on unsteady Casson magneto-nanofluid flow over an inclined plate embedded in a porous medium. *World Journal of Engineering*, *16*(2), 260-274. https//dio. Org/10.1108/WJE-04-2018-0144.
3. Aman, S., Khan, I., Ismail, Z., Salleh, M. Z., Alshomrani, A. S., & Alghamdi, M. S. (2017). Magnetic field effect on Poiseuille flow and heat transfer of carbon nanotubes along a vertical channel filled with Casson fluid. *AIP Advances*, *7*(1), 015036.
4. Aman, S., Khan, I., Ismail, Z., Salleh, M. Z., & Tlili, I. (2018). A new Caputo time fractional model for heat transfer enhancement of water based graphene nanofluid: An application to solar energy. *Results in physics*, *9*, 1352-1362.
5. Abbas, Z., Hussain, S., Rafiq, M. Y., & Hasnain, J. (2020). Oscillatory slip flow of Fe3O4 and Al2O3 nanoparticles in a vertical porous channel using Darcy's law with thermal radiation. *Heat Transfer*, *49*(6), 3228-3245. https://doi.org/10.1002/htj.21771
6. Sobamowo, M. G. (2018). Combined effects of thermal radiation and nanoparticles on free convection flow and heat transfer of casson fluid over a vertical plate. *International Journal of*

Chemical Engineering, *2018*. https://doi.org/10.1155/2018/7305973

7. Das, K., Sarkar, A., & Kundu, P. K. (2017). Nanofluid flow over a stretching surface in presence of chemical reaction and thermal radiation: an application of Lie group transformation. *Журнал Сибирского федерального университета. Серия «Математика и физика»*, *10*(2), 146-157.
8. Muhammad, T., Waqas, H., Manzoor, U., Farooq, U., & Rizvi, Z. F. (2022). On doubly stratified bioconvective transport of Jeffrey nanofluid with gyrotactic motile microorganisms. *Alexandria Engineering Journal*, *61*(2), 1571-1583.
9. Hayat, T., Qayyum, S., & Alsaedi, A. (2017). Mechanisms of nonlinear convective flow of Jeffrey nanofluid due to nonlinear radially stretching sheet with convective conditions and magnetic field. *Results in physics*, *7*, 2341-2351.
10. Reddy, M. G., & Makinde, O. D. (2016). Magnetohydrodynamic peristaltic transport of Jeffrey nanofluid in an asymmetric channel. *Journal of Molecular Liquids*, *223*, 1242-1248.
11. Waqas, M., Shehzad, S. A., Hayat, T., Khan, M. I., & Alsaedi, A. (2019). Simulation of magnetohydrodynamics and radiative heat transport in convectively heated stratified flow of Jeffrey nanofluid. *Journal of Physics and Chemistry of Solids*, *133*, 45-51.
12. Abbasi, F. M., Shehzad, S. A., Hayat, T., & Alhuthali, M. S. (2016). Mixed convection flow of jeffrey nanofluid with thermal radiation and double stratification. *Journal of Hydrodynamics, Ser. B*, *28*(5), 840-849.
13. Ahmad, B., Nawaz, A., Smida, K., Khan, S. U., Khan, M. I., Abbas, T., ... & Galal, A. M. (2022). Thermal diffusion of Maxwell nanoparticles with diverse flow features: Lie group simulations. *International Communications in Heat and Mass Transfer*, *136*, 106-164.
14. Jha, B. K., & Samaila, G. (2023). Nonlinear approximation for buoyancy-driven mixed convection heat and mass transfer flow over an inclined porous plate with Joule heating, nonlinear thermal radiation, viscous dissipation, and thermophoresis effects. *Numerical Heat Transfer, Part B: Fundamentals*, *83*(4), 139-161. DOI: 10.1080/10407790.2022.2150341.
15. Khan, M. I., Waqas, M., Hayat, T., Alsaedi, A., & Khan, M. I. (2017). Significance of nonlinear radiation in mixed convection flow of magneto Walter-B nanoliquid. *International Journal of Hydrogen Energy*, *42*(42), 26408-26416.
16. Ilias, M. R., Ismail, N. S. A., AbRaji, N. H., Rawi, N. A., & Shafie, S. (2020). Unsteady aligned MHD boundary layer flow and heat transfer of a magnetic nanofluids past an inclined plate. *International Journal of Mechanical Engineering and Robotics Research*, *9*(2), 197-206.
17. Hayat, T., Mustafa, M., & Pop, I. (2010). Heat and mass transfer for Soret and Dufour's effect on mixed convection boundary layer flow over a stretching vertical surface in a porous medium filled with a viscoelastic fluid. *Communications in Nonlinear Science and Numerical Simulation*, *15*(5), 1183-1196.
18. Turkyilmazoglu, M. (2013). The analytical solution of mixed convection heat transfer and fluid flow of a MHD viscoelastic fluid over a permeable stretching surface. *International Journal of Mechanical Sciences*, *77*, 263-268.